Synthesis of Molybdenum Oxide Nanoplatelets during Crystallization of the Precursor Gel from Its Hybrid Nanocomposites

Guan Wang,*,† Yuan Ji,† Lihua Zhang,‡ Yimei Zhu,‡ Pelagia-Irene Gouma,† and Michael Dudley†

Department of Materials Science and Engineering, Stony Brook University, Stony Brook, New York 11794, and Department of Materials Science, Brookhaven National Laboratory, Upton, New York 11973

Received October 13, 2006
Revised Manuscript Received December 21, 2006

Nanostructured metal oxides with reduced dimensionality (nanotubes,[1,2] nanowires,[3,4] nanorods,[5,6] and nanobelts[7,8]) and their applications have been attracting considerable attention. Characterized by their high aspect ratio, nearly perfect crystallinity, structural anisotropy, and small tip radii of curvatures, nanostructured oxides are expected to have remarkable optical, electrical, magnetic, and ionic transport properties.[7,9−11] Therefore, fabrication of crystalline metal oxides with lowered dimensionality can often lead to innovative properties and applications. However, it is still a challenge to explore new approaches to tailor the dimensionality and geometry of the oxides with high crystallinity and purity.

As a wide band gap n-type semiconductor, molybdenum oxide (MoO_3) is one of the most intriguing transition metal oxides.[12] It has been widely used in industry as photochromic and electrochromic devices,[13,14] gas sensors,[15] and catalysts.[16] In addition, it has been found to be a good precursor for the synthesis of many other important compounds.[17−19] Of the same interest is the peculiar layered structure of α-MoO_3,[20,21] the most common form of crystalline molybdenum oxides, which offers rich intercalation chemistry. Efforts have been devoted to the preparation of ordered hierarchical arrangement of organic−inorganic composites with layered α-MoO_3 as the host material.[22−24] Conversion of crystalline MoO_3 powder to nanofibers and nanobelts by the hydrothermal method and subsequent thermal treatment have also been realized.[25] To our best knowledge, there is still no report on the morphological organization of molybdenum oxide synthesized directly from its amorphous state with a high purity.

Sol−gel chemistry is widely used to synthesize a variety of nanostructured oxides based on the polymerization of molecular precursors via wet chemical methods.[26] The hydrolysis reaction of appropriate alkoxides often results in the formation of oxides with amorphous or metastable phases, which are not produced by other synthesis routes. In addition, the mild chemical conditions allowed by the sol−gel process provide a versatile access to form hybrid organic−inorganic nanocomposites. The degree of interpenetration of the organic and inorganic components can be adjusted from the submicrometer range down to the nanometer scale.[27]

Herein, we report on a simple method that has successfully realized the shape-controlled growth of crystalline molybdenum oxide. Large scale α-MoO_3 nanoplatelets have been yielded without the use of any catalyst. This method exploits the combination of the surfactant/inorganic self-assembly process and host/guest intercalation chemistry to obtain anisotropic crystallization of the molybdenum oxide directly from its amorphous gel. A model has been proposed to explain the formation mechanism of the two-dimensional (2D) MoO_3 nanoplatelets. This method is effective, easily controllable and may be applied widely for the production of other 2D nanostructures.

The molybdenum oxide gel was made by using molybdenum isopropoxide ($Mo(OC_3H_7)_5$, Chemat) as the precursor, which was dissolved into 1-butanol to form a 0.2 M solution. After mechanically agitating for 5 min, the solution was ultrasonicated for 2 h and then aged in a closed container for 24 h. A clear blue gel was obtained after aging. The typical blue color indicated the coexistence of different Mo oxidation states, whose relative amount and evolution at elevated temperatures depend on the material typology.[28] On

* To whom correspondence should be addressed. E-mail: guwang@ic.sunysb.edu.
† Stony Brook University.
‡ Brookhaven National Laboratory.

(1) Tenne, R.; Margulis, L.; Genut, M.; Hodes, G. *Nature* **1992**, *360*, 444.
(2) Rao, C. N. R.; Govindaraj, A.; Deepak, F. L.; Gunari, N. A.; Nath, M. *Appl. Phys. Lett.* **2001**, *78*, 1853.
(3) Morales, A. M.; Lieber, C. M. *Science* **1998**, *279*, 208.
(4) Duan, X. F.; Lieber, C. M. *Adv. Mater.* **2000**, *12*, 298.
(5) Yu, Y. Y.; Chang, S. S.; Lee, C. L.; Wang, C. R. C. *J. Phys. Chem. B* **1997**, *101*, 6661.
(6) Manna, L.; Scher, E. C.; Alivisatos, A. P. *J. Am. Chem. Soc.* **2000**, *122*, 12700.
(7) Pan, Z. W.; Dai, Z. R.; Wang, Z. L. *Science* **2001**, *291*, 1947.
(8) Arnold, M. S.; Avouris, P.; Pan, Z. W.; Wang, Z. L. *J. Phys. Chem. B* **2003**, *107*, 659.
(9) Hu, J. T.; Odom, T. W.; Lieber, C. M. *Acc. Chem. Res.* **1999**, *32*, 435.
(10) Patzke, G. R.; Krumeich, F.; Nesper, R. *Angew. Chem., Int. Ed.* **2002**, *41*, 2446.
(11) Li, Y. B.; Bando, Y.; Golberg, D.; Kurashima, K. *Appl. Phys. Lett.* **2002**, *81*, 5048.
(12) Hussain, Z. *J. Mater. Res.* **2001**, *16*, 2695.
(13) Yao, J. N.; Hashimoto, K.; Fujishima, A. *Nature* **1992**, *355*, 624.
(14) Yang, Y. A.; Cao, Y. W.; Loo, B. H.; Yao, J. N. *J. Phys. Chem. B* **1998**, *102*, 9392.
(15) Taurino, A. M.; Forleo, A.; Francioso, L.; Siciliano, P.; Stalder, M.; Nesper, R. *Appl. Phys. Lett.* **2006**, *88*.
(16) Liu, H. F.; Liu, R. S.; Liew, K. Y.; Johnson, R. E.; Lunsford, J. H. *J. Am. Chem. Soc.* **1984**, *106*, 4117.
(17) Margulis, L.; Salitra, G.; Tenne, R.; Talianker, M. *Nature* **1993**, *365*, 113.
(18) Hershfinkel, M.; Gheber, L. A.; Volterra, V.; Hutchison, J. L.; Margulis, L.; Tenne, R. *J. Am. Chem. Soc.* **1994**, *116*, 1914.
(19) Zach, M. P.; Ng, K. H.; Penner, R. M. *Science* **2000**, *290*, 2120.
(20) Andersson, G.; Magneli, A. *Acta Chem. Scand.* **1950**, *4*, 793.
(21) McCarron, E. M. *J. Chem. Soc., Chem. Commun.* **1986**, 336.
(22) Tagaya, H.; Ara, K.; Kadokawa, J.; Karasu, M.; Chiba, K. *J. Mater. Chem.* **1994**, *4*, 551.
(23) Nazar, L. F.; Wu, H.; Power, W. P. *J. Mater. Chem.* **1995**, *5*, 1985.
(24) Hosono, K.; Matsubara, I.; Murayama, N.; Woosuck, S.; Izu, N. *Chem. Mater.* **2005**, *17*, 349.
(25) Song, R. Q.; Xu, A. W.; Deng, B.; Fang, Y. P. *J. Phys. Chem. B* **2005**, *109*, 22758.
(26) Brinker, C. J.; Scherer, G. W. *Sol-Gel Science: The Physics and Chemistry of Sol-Gel Processing*; Academic Press, Inc.: San Diego, 1990.
(27) Sanchez, C.; Ribot, F. *New J. Chem.* **1994**, *18*, 1007.
(28) Epifani, M.; Imperatori, P.; Mirenghi, L.; Schioppa, M.; Siciliano, P. *Chem. Mater.* **2004**, *16*, 5495.

10.1021/cm062454m CCC: $37.00
Published on Web 02/14/2007

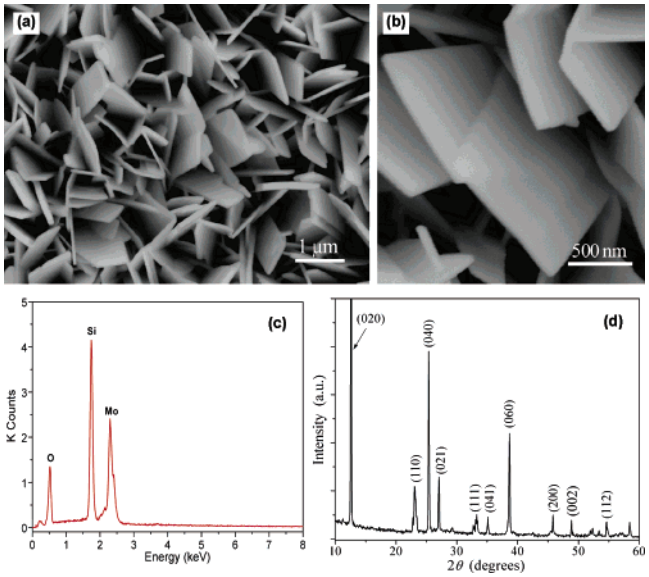

Figure 1. SEM images of the MoO_3 nanoplatelets under magnifications of (a) 30 K and (b)80 K, (c) EDS pattern of the nanoplatelets (Si peak originated from the substrate), and (d) XRD of the nanoplatelet sample on Si.

the other hand, poly(ethylene oxide) (PEO, molecular weight = 400 000, Aldrich) was dissolved in ethanol by continuously stirring at 50 °C to form a viscous solution with a concentration of 0.05 g/mL. This solution was mixed with the molybdenum oxide sol in the volume ratio of 1:1. Nanocomposite film was formed on the Si substrate by the dip-coating method. The film was left in air for 3 days. The same dip-coating process was repeated three times. A fully hydrolyzed film was obtained. Then the composite film was calcined up to 500 °C at a heating rate of 2 °C/min, to obtain crystallized molybdenum oxide and remove the polymer. The samples were characterized with a field emission scanning electron microscope (FESEM, LEO 1550) equipped with energy dispersive X-ray spectroscopy (EDS), high-resolution transmission electron microscopy (HRTEM, JEOL JEM 3000F), and X-ray diffraction (XRD). The in situ XRD data were recorded using a position sensitive detector (PSD) while heating the sample within the X-ray beam from 25 °C to 525 °C.

FESEM images showed that as-prepared products after calcination were mainly composed of nanoplatelets with regular shape, as illustrated in Figure 1a,b. Most nanoplatelets have nearly rectangular shape about 1−2 μm across. The thicknesses of the nanoplatelets range from tens of nanometers to around 100 nanometers. The energy dispersive spectrum for samples deposited on the Si wafer confirmed that the nanoplatelets consisted only of oxygen and molybdenum (see Figure 1c). The XRD pattern of this sample provided clear evidence of the crystalline structure (see Figure 1d). The diffraction peaks could be readily indexed to the orthorhombic phase of MoO_3 (*Pbnm*, JCPDS no. 05-0508) with the lattice parameters $a = 3.962$ Å, $b = 13.858$ Å, and $c = 3.697$ Å. For a sample deposited on Si wafer, much stronger diffraction intensities have been found from the (0*k*0) peaks, suggesting the anisotropic growth of the nanoplatelets. The preferential orientation in the [010] direction is due to their planar geometry.

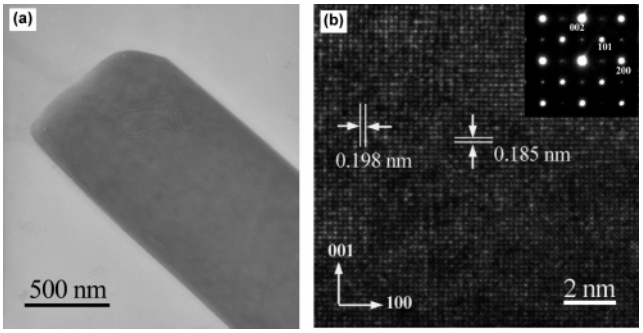

Figure 2. (a) TEM image of a single MoO_3 nanoplatelet; (b) HRTEM image of the nanoplatelet and the corresponding SAED (inset).

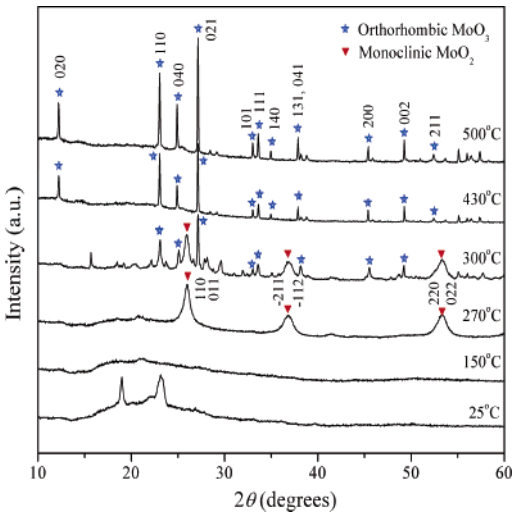

Figure 3. Representative in situ XRD patterns showing the dynamic structure evolution of the nanoplatelets from the hybrid nanocomposites.

Figure 2a presents a typical TEM image for a single MoO_3 nanoplatelet. The nanoplatelet showed a uniform contrast, which is a general feature of all individual nanoplatelets. The selected area electron diffraction (SAED) pattern of the sample was recorded perpendicular to the planar facet (see Figure 2b, inset). The pattern agreed well with the [010] zone axis diffraction of the orthorhombic MoO_3, as reported in the literature.[11,29] We employed SAED on different parts of the sample. The same SAED patterns were observed, implying that the nanoplatelet is single crystalline. HRTEM images of the sample showed two sets of parallel fringes with a spacing of 1.98 Å and 1.85 Å, corresponding to (200) and (002) planes, respectively (see Figure 2b). HRTEM indicated a high degree of crystallinity of the sample, while there was still some disorder, which might be induced by the existence of oxygen vacancies.

To understand the dynamic structure transformation of the MoO_3 nanoplatelets from their nanocomposites, in situ XRD was carried out by using synchrotron X-ray as the incidence beam. A continuous phase transformation has been observed. Typical diffraction patterns at specific temperatures have been shown in Figure 3. The XRD pattern of the nanocomposites was recorded at 25 °C. Two broad peaks near 19° and 23° came from characteristic diffraction of semicrystalline PEO. As temperature increased above the glass

(29) Xia, T. A.; Li, Q.; Liu, X. D.; Meng, J. A.; Cao, X. Q. *J. Phys. Chem. B* **2006**, *110*, 2006.

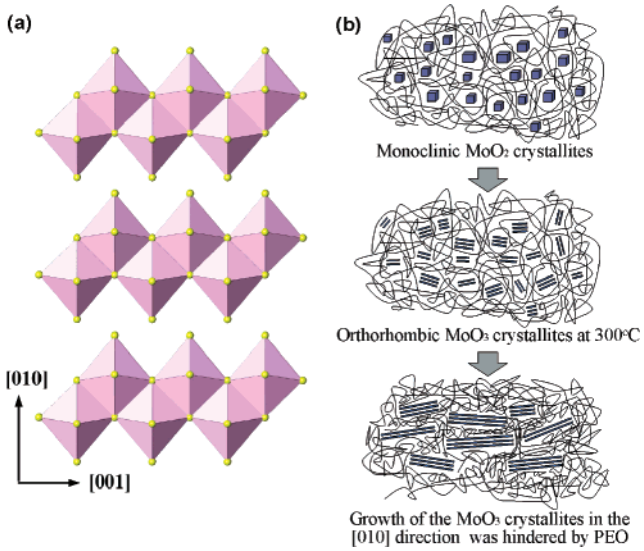

Figure 4. (a) Layer structure of α-MoO_3 and (b) proposed crystallization process for the formation of MoO_3 nanoplatelets.

transition temperature of PEO (65 °C), no diffraction peak was observed, implying an amorphous characteristic of the hydrolysis product from the sol−gel precursor. Three broad peaks occurred at 270 °C. They could be indexed to monoclinic MoO_2 (*P*21/*c*, JCPDS no. 78-1072). According to the full width at half-maximum of the peaks, the crystalline size was calculated to be around 10 nm. An obvious phase transformation from monoclinic MoO_2 to orthorhombic MoO_3 started from 300 °C. A mixture of two phases was found from the in situ XRD pattern. Some weak peaks which could not be indexed were believed to be from the intermediate compounds during the transition. A pure orthorhombic phase was obtained at 430 °C. This phase was stable up to 500 °C, indexed to the same α-MoO_3 structure (*Pbnm*, JCPDS no. 05-0508) as in Figure 1d. Preferential diffraction disappeared in the in situ XRD pattern because of the different geometry of the sample while collecting the diffraction data.

On the basis of the in situ XRD results and thermal analysis of the nanocomposites (see Supporting Information), a model has been proposed to explain the formation mechanism of the crystalline MoO_3 nanoplatelets. It is well-known that α-MoO_3 has vertex-sharing chains of distorted MoO_6 octahedra, which share edges with other similar chains to form layers (see Figure 4a). These 2D sheets are weakly held together by van der Waals forces, so they can be readily propped open by intercalation species. Crystal growth in the [010] direction is more like the assembling of the layer structure. We suggest that the crystallization of molybdenum oxide from its polymer nanocomposites started from the formation of tiny MoO_2 crystallites, which were distributed uniformly among the polymer chains. As *T* increased above 300 °C, MoO_2 transformed to MoO_3 layer-structured crystallites immediately, which were still surrounded by polymer chains. The in-plane crystal growth of MoO_3 involved the formation of Mo−O bonds with a large energy release during this process. Meanwhile, the inter-plane region was intercalated effectively by the polymer surfactant. Since crystal growth in the inter-plane direction has to overcome the intercalation effect of the polymer, it is not energetically preferred. At 500 °C, PEO decomposed completely, and crystalline orthorhombic MoO_3 formed with an anisotropic geometry.

Several factors can affect the growth of the MoO_3 nanoplatelets from the hybrid nanocomposites, including the sol−gel concentration, type and concentration of polymer, heating rate and temperature, and so forth. We have demonstrated that other polymer surfactants, such as poly(vinyl pyrrolidone) (PVP), can play the same role as PEO (see Supporting Information). Similar MoO_3 nanoplatelets have been produced without changing any other conditions. Investigations of the effects of other factors are in progress.

In summary, we have successfully synthesized MoO_3 nanoplatelets from the molybdenum oxide sol−gel and polymer hybrid nanocomposites. All the nanoplatelets showed a lowered dimensionality in the [010] direction. Detailed TEM analysis revealed that the nanoplatelets were single crystal of flat face with good crystallinity. In situ XRD illustrated the dynamic structural formation of the orthorhombic MoO_3 nanoplatelets. The function of polymer as the surfactant and intercalation material during the crystallization of the layer structure of MoO_3 has been discussed, interpreting the preferential growth of the nanoplatelets from the nanocomposites. This method may be applied to the growth of low dimensional structures of other materials with layered structure.

Acknowledgment. This project has been supported by a National Science Foundation (NSF) NIRT Grant (award ID: 0304169). The in situ XRD experiments have been carried out at Beamline X18A at the National Synchrotron Light Source (NSLS), Brookhaven National Laboratory (BNL), which is supported by the U.S. Department of Energy (D.O.E.). HRTEM work was supported by the U.S. Department of Energy, Division of Materials, Office of Basic Energy Science, under Contract No. DE-AC02-98CH10886. G.W. is grateful for the generous help from Dr. Xiaoqing Yang and Dr. Jonathan Hanson at BNL with the XRD experiments.

Supporting Information Available: Differential scanning calorimetry and thermogravimetric analysis of the molybdenum oxide sol−gel and PEO nanocomposites (Figure S1) and SEM (Figure S2) and XRD (Figure S3) of the MoO_3 nanoplatelets prepared with PVP as the polymer surfactant (PDF). This material is available free of charge via the Internet at http://pubs.acs.org.

CM062454M